

SINGLE SNEUTRINO PRODUCTION AND THE WRONG CHARGED LEPTON SIGNAL

St. Kolb, M. Hirsch[†], H.V. Klapdor-Kleingrothaus and O. Panella[‡]

Max-Planck-Institut für Kernphysik, P.O. 10 39 80, D-69029 Heidelberg, Germany

[†]*Department of Physics and Astronomy, University of Southampton, Highfield, Southampton
SO17 1BJ, England*

[‡]*Istituto Nazionale di Fisica Nucleare, Sezione di Perugia, Via A. Pascoli, I-06123 Perugia, Italy*

(February 8, 2020)

Abstract

Lepton number violation could be manifest in the sneutrino sector of supersymmetric extensions of the standard model. Then sneutrinos decay partly into the “wrong sign lepton” final state, if kinematically accessible. At a future electron-positron Linear Collider facility or an electron-photon facility this signal could be directly visible in associated single sneutrino production mechanisms, if sneutrino pair production is not possible. Under favourable circumstances, for the projected luminosity of the Next Linear Collider the rate of the wrong sign lepton signal may be of order $\mathcal{O}(10/\text{year})$ for a sneutrino mass-splitting and sneutrino widths of order $\mathcal{O}(1 \text{ GeV})$.

12.60.Jv, 12.60.-i, 14.80.Ly, 11.30.Fs

I. INTRODUCTION

Recently there has been special interest in the bosonic counterpart of the neutrino appearing in supersymmetric (SUSY) extensions of the Standard Model [1], the sneutrino. This is due to the intimate relation of neutrino and sneutrino properties as regards the violation of the lepton number L : either both neutrino and sneutrino violate L or both do not [2]. If L is violated, the sneutrino states in one generation exhibit a mass-splitting $\Delta m = m_1 - m_2$, independent of the precise mechanism which generates L violation in the sneutrino sector. The masses $m_{1,2}$ correspond to the mass states $\tilde{\nu}_\ell^N$, $N=1,2$ (without mixing in generation space, ℓ denotes generation) which (in the effective low-energy theory) are the physical states instead of the weak interaction states $\tilde{\nu}_L(\ell), \tilde{\nu}_L^*(\ell)$ (degenerate in mass in the absence of L violation) [2,3]. For the masses $m_{1,2}$ the relation $m_{1,2} = \bar{m} \pm \Delta m/2$ holds, where $\bar{m} = (m_1 + m_2)/2$ is the average sneutrino mass. The amount of L -violation (Δm) is restricted by the kinematical upper limits on neutrino masses and neutrinoless double beta decay [4,5]: the limit on Δm is very stringent for the first generation, but leaves room for appreciable L violation for the second and third generation (see section II). If the electroweak phase transition is weakly first or second order, another constraint is set by baryogenesis [6].

Besides possibly observable phenomena in future collider experiments [7], L violation implies that the lightest sneutrino state may become the lightest supersymmetric particle (LSP) and - if its mass is around 70 GeV - a candidate for the cold dark matter in the universe [8]. This case should be easily discernable at a future lepton collider facility [9]. In the absence of L violation the sneutrino cannot account for the cold dark matter in the universe [10,11]. In the opposite case of heavy sneutrinos, L -violation in the sneutrino sector could manifest itself by a wrong sign lepton stemming from the decay of a sneutrino in a lepton and a chargino [4,3].

In view of the low energy constraints on the mass-splitting the discussion will be focussed on second and third generation sneutrinos. Several production mechanisms may be of interest to produce sneutrinos at an e^+e^- machine, depending on the mass relations of the

sneutrinos with respect to the other particles of the SUSY spectrum, especially the chargino. The most obvious production channel is pair production: $e^+e^- \rightarrow \tilde{\nu}_\ell^1 \tilde{\nu}_\ell^2$ in the L -violating case or $e^+e^- \rightarrow \tilde{\nu}_L(\ell) \tilde{\nu}_L^*(\ell)$ in the L -conserving case.

If however sneutrino pair production is kinematically not accessible, *single* sneutrino production has to be considered in order to gain some insight into the sneutrino properties. Examples of processes, where a single sneutrino of any flavour is produced at *e.g.* a future electron positron Linear Collider (LC) [12] or at an accompanying electron-photon collider [13], are:

$$e^+e^- \rightarrow \tilde{\nu}_\ell^N \ell^\pm \chi_k^\mp \quad (1a)$$

$$e^+\gamma \rightarrow \tilde{\nu}_\ell^N \bar{\nu}_\ell \tilde{\ell}^+ \quad (1b)$$

$$e^+e^- \rightarrow \tilde{\nu}_\ell^N W^\pm \tilde{\ell}^\mp, \quad (1c)$$

where $k=1,2$ and χ_2^\pm is the lighter of the two chargino states. In the presence of L violation the electric charge of the lepton produced in the decay of sneutrinos (assumed heavier than charginos)

$$\tilde{\nu}_\ell^N \rightarrow \ell^\pm \chi^\mp \quad (2)$$

may be of the wrong sign compared to the L -conserving case. In the following, the “wrong sign charged lepton” will be used as a signal for L violation.

The processes in eq. (1a,1b) can be regarded as the leptonic SUSY analogues of single top-quark production [14] in the SM. It should also be recalled that sneutrinos can in addition be produced with accompanying neutrinos and neutralinos, *e.g.* by the process $e^+e^- \rightarrow \tilde{\nu}_\ell^N \nu_\ell \chi_k^0$, resulting in a final state very difficult to observe or not observable at all. Hence this possibility will not be considered further.

As the aim of this work is largely exploratory the attention is focussed on the value of total cross sections which are estimated at the energies of a future e^+e^- linear collider

(LC). Kinematic cuts, which may be specific of the particular detector and/or experiment are not included. These can only be implemented in a realistic MonteCarlo simulation of the signal with a parallel detailed study of the background which is however beyond the scope of this work. Nonetheless in order to have an idea of the observability of such phenomena the estimated total cross sections are compared to the prospected luminosity of a future LC which for the TESLA project are as follows [15]: at $\sqrt{s} = 500$ GeV, $\mathcal{L}_o = 3 \times 10^{34} \text{ cm}^{-2}\text{sec}^{-1}$ while the integrated luminosity over a period of one year (10^7sec) is $L_o = 300 \text{ fb}^{-1}$; at $\sqrt{s} = 800$ GeV, $\mathcal{L}_o = 5 \times 10^{34} \text{ cm}^{-2}\text{sec}^{-1}$ and $L_o = 500 \text{ fb}^{-1}$. It is also expected that the LC will be able to operate in the electron-photon ($e^-\gamma$), photon-photon ($\gamma\gamma$) and electron-electron (e^-e^-) modes with luminosities comparable to that of the underlying e^+e^- machine (even higher in the case of the $\gamma\gamma$ mode) [16].

The topic of this note is to discuss the prospects of detection of the wrong sign lepton signal if sneutrinos are heavy and pair production is kinematically excluded. In view of the low energy constraints on the mass-splitting the discussion will be focussed on second and third generation sneutrinos. Throughout this note it will be assumed that R -parity is conserved. For a discussion of the effects of R -parity violation see refs. [3,17].

In the next section the reaction in eq. (1a) will be considered, and in section III the process in eq. (1b) will be analyzed. For both cases the cross section of the wrong charged lepton signal will be estimated. The reaction in eq. (1c) produces a more difficult signature due to the additional W boson in the final state and therefore will not be analyzed.

II. THE REACTION $e^+e^- \rightarrow \chi^\pm \tilde{\nu}_\ell^N \ell^\mp$, $\ell = \mu, \tau$

The Feynman graphs contributing to this reaction are depicted in Fig. 1 if the flavour of the final state sneutrino is either $\ell=\mu$ or $\ell=\tau$. If $\ell=e$, then further contributions similar to those examined in [18] (replacing the proton with an electron) have to be taken into account. The resulting cross-section can be written as

$$\sigma^{tot} = \sum_{k,l=I; k \leq l}^{III} \sigma^{(k,l)} \quad (3)$$

where *e.g.* $\sigma^{I,II}$ is the contribution from the interference of s -channel gauge boson exchange (Fig. 1-I) and t -channel sneutrino exchange (Fig. 1-II). The explicit expressions of the various contributions are listed in appendix A.

Since the graph in Fig. 1-III contains the derivative coupling of the Z^0 to the sneutrinos, its contribution is β -suppressed and always much smaller than the modes in Figs. 1-I and 1-II. Therefore, in the following it is neglected.

The three-particle phase space integral of graphs can be split into two two-particle phase space integrals (see *e.g.* [19]), so that the phase space integrals relative to the contributions in Fig. 1-I and 1-II (and their interference) can be evaluated analytically up to the integration over Q^2 to be integrated numerically, where Q is the sum of the lepton and chargino impulses. We have checked, that using the small width approximation $1/(x^2 + \epsilon^2) \approx \pi\delta(x)/\epsilon$ (for $\epsilon \ll x$) the three body cross-sections $\sigma^{(III,III)}$ and $\sigma^{(I,I)+(II,II)+(I,II)}$ simplify in factorised expressions of the sneutrino and chargino pair production times the corresponding sneutrino and chargino partial decay width if kinematically allowed.

If the final state sneutrino is lighter than at least one of the charginos, the cross-section depends very sensitively on the chargino width. However, in what follows the sneutrino will be taken to be heavier than both charginos and their width will be neglected. In Fig. 3 the cross section eq. (3) is plotted in terms of the final state sneutrino mass (which in principle could be different from the mass entering the propagator, but this has not been taken into account) for two sets of SUSY parameters $\mu, M_2, \tan\beta$ (μ is the Higgs mixing parameter, M_2 is the gaugino mass associated to $SU(2)_L$, and $\tan\beta$ is the ratio of the vacuum expectation values of the two Higgs doublets) defined in tab. I and for beam energies $\sqrt{s}=500$ GeV and $\sqrt{s}=800$ GeV. In the following the unification condition in a minimal supergravity (mSUGRA) model $M_1=(5/3)M_2 \times \tan^2\Theta_W$ is assumed unless stated otherwise. In the sneutrino mass region where sneutrino pair production is kinematically excluded the cross section is of order 0.1 fb or lower.

In order to estimate the cross section for the L-violating wrong sign lepton signal we introduce the L-violating sneutrino propagator [2]

$$\langle 0|T[\tilde{\nu}(x)\tilde{\nu}(y)]|0\rangle = \Delta m^2 \frac{i}{2} \int \frac{d^4 k}{(2\pi)^4} \frac{e^{-ik(x-y)}}{(m_1^2 - k^2)(m_2^2 - k^2) + i\epsilon} \quad (4)$$

and use the small width approximation. The cross section eq. (3) becomes:

$$\sigma^{L-viol.} = \xi \left[\sigma^{tot}(\tilde{\nu}^1) \frac{\Gamma(\tilde{\nu}^1 \rightarrow \chi^\pm \ell^\mp)}{\Gamma^{tot}(\tilde{\nu}^1)} \Theta(m_1^2 - \bar{s}_-) \Theta(\bar{s}_+ - m_1^2) + \sigma^{tot}(\tilde{\nu}^2) \frac{\Gamma(\tilde{\nu}^2 \rightarrow \chi^\pm \ell^\mp)}{\Gamma^{tot}(\tilde{\nu}^2)} \Theta(m_2^2 - \bar{s}_-) \Theta(\bar{s}_+ - m_2^2) \right], \quad (5)$$

where

$$\bar{s}_+ = \sqrt{s} - m_{\chi_2} - m_\ell, \quad \bar{s}_- = m_{\chi_1} + m_\ell.$$

The definition of \bar{s}_- implies that the light sneutrino state contributes only if it is heavier than both charginos. Otherwise the light sneutrino may be produced by the decays of a real chargino and the width has to be taken into account (see the comment above). The L-violating factor ξ is defined as

$$\xi = \frac{(\Delta m^2)^2 + [m_2 \Gamma^{tot}(\tilde{\nu}^2) - m_1 \Gamma^{tot}(\tilde{\nu}^1)]^2}{(\Delta m^2)^2 + m_1^2 [\Gamma^{tot}(\tilde{\nu}^1)]^2 + m_2^2 [\Gamma^{tot}(\tilde{\nu}^2)]^2}, \quad 0 \leq \xi \leq 1. \quad (6)$$

The behaviour of ξ in dependence on the sneutrino mass-splitting divided by the average sneutrino mass ($\Delta m/\overline{m}$) is illustrated in Fig. 4. Since it is assumed that the sneutrino is heavier than both charginos, the sneutrino width is estimated taking into account only two body decay modes

$$\tilde{\nu}_\ell^{1,2} \rightarrow \ell^\pm \chi_j^\mp, \quad \tilde{\nu}_\ell^{1,2} \rightarrow \nu \chi_j^0. \quad (7)$$

For the parameters chosen in tab. I the difference between the average sneutrino mass and the charged slepton mass is smaller than the mass of the weak gauge bosons. However, for a large mass-splitting the heavier sneutrino may decay as $\tilde{\nu}_\ell^1 \rightarrow \tilde{\ell}^\pm + W^\mp$. Since the charged slepton usually decays with a large branching fraction into a neutralino-lepton final state, the L-violating signal would be slightly enhanced.

The L-violating signal is a very clear one (see below), therefore it is reasonable to assume that few events per year should be sufficient for signal detection and for an integrated luminosity of order $\mathcal{O}(\text{few} \times 100 \text{ fb}^{-1})$ a cross section as small as $\mathcal{O}(0.01 \text{ fb})$ could be measured. In Fig. 5 the cross section for the L-violating signal is plotted versus the relative sneutrino mass-splitting ($\Delta m/\bar{m}$) for the parameter sets as defined in tab. I and for different values of the average sneutrino mass. The dominant contribution comes always from the lighter sneutrino state, and in extending the amount of L-violation it has been made sure that the lighter sneutrino is sufficiently heavy so that the widths of both charginos may be safely neglected.

In the cases ($\bar{m}=275 \text{ GeV}$; $\sqrt{s}=500 \text{ GeV}$; set A) and ($\bar{m}=450 \text{ GeV}$; $\sqrt{s}=800 \text{ GeV}$; sets A and B) a relative mass-splitting $\Delta m/\bar{m}$ of order $\mathcal{O}(0.01)$ is sufficient to produce an L-violating cross section of order $\mathcal{O}(0.01 \text{ fb})$. For the remaining cases ($\bar{m}=350 \text{ GeV}$; $\sqrt{s}=500 \text{ GeV}$; set A) and ($\bar{m}=600 \text{ GeV}$; $\sqrt{s}=800 \text{ GeV}$; sets A and B) the relative mass-splitting has to be one or two orders of magnitude larger in order to produce a visible signal.

The curves plotted in Fig. 5 should be compared to the low-energy limits on the sneutrino mass-splitting. Loops containing L-violating sneutrinos and neutralinos contribute to the Majorana neutrino mass matrix \mathcal{M}_{LL} mixing the $SU(2)_L$ doublet fields [4,5,3]. In ref. [5] a scan over a large range of the SUSY parameter space has been carried out and the following “absolute” limit has been derived from the upper limits on neutrino masses:

$$\Delta m(\ell) < 156 \frac{m_{\nu}^{exp}(\ell)}{1 \text{ eV}} \text{ keV} , \quad (8)$$

where \bar{m} has been set to 100 GeV. Higher values for \bar{m} result in less stringent bounds. In the cases ($\bar{m}=275 \text{ GeV}$; $\sqrt{s}=500 \text{ GeV}$; set A) and ($\bar{m}=450 \text{ GeV}$; $\sqrt{s}=800 \text{ GeV}$; sets A and B) a neutrino mass of order $\mathcal{O}(10 \text{ keV})$ would be compatible with a relative sneutrino mass difference of order $\mathcal{O}(0.01)$. The current kinematical limits on neutrino masses are [20]

$$m_{\nu}^{exp}(e) < 3 \text{ eV} , \quad m_{\nu}^{exp}(\mu) < 190 \text{ keV} , \quad m_{\nu}^{exp}(\tau) < 18.2 \text{ MeV} ,$$

i.e. the kinematical limits leave room for an observable sneutrino mass-splitting in the second and third generation. On the other hand, the limit on the m_{ee} entry of \mathcal{M}_{LL} from

the Heidelberg-Moscow $0\nu\beta\beta$ -decay experiment [21] together with the preliminary results of neutrino oscillation experiments (for a recent overview see *e.g.* [22]) imply that all entries of \mathcal{M}_{LL} should satisfy $m_{ij} \lesssim 2.5$ eV [23]. If the oscillation solution (requiring mass-squared differences between the neutrino states of order $\mathcal{O}(1 \text{ eV}^2)$ or less) will be confirmed both for the atmospheric and for the solar neutrino problem, sneutrino-induced L violation will not be directly visible for sneutrino decay widths of order $\mathcal{O}(1 \text{ GeV})$. If, on the other hand, the oscillation solution to one or both of the neutrino problems are not confirmed, several entries of \mathcal{M}_{LL} are no longer required to be small, and neutrinos could still be much heavier than currently accepted.

Furthermore, it has been pointed out in ref. [3] that sneutrino oscillations could be observable even for neutrino masses of order $\mathcal{O}(1 \text{ eV})$ provided that the total decay widths of the sneutrino mass states are very small. In the approach taken here this means that ξ is of order $\mathcal{O}(1)$ for very small values of Δm . For example, for a neutrino mass of 1 eV (corresponding to $\Delta m = 156 \text{ keV}$) the L-violating cross section for set A and $\sqrt{s}=500 \text{ GeV}$ is of order $\mathcal{O}(0.01 \text{ fb})$ provided that the sneutrino widths are of order $\mathcal{O}(1 \text{ MeV})$. This fact is illustrated in Fig. 6, where the sneutrino width has been varied freely. Such tiny sneutrino widths are conceivable for a small mass difference of sneutrinos in respect to the lighter chargino and the LSP neutralino (still it has to be made sure that the final state leptons are not too soft to be detectable). This is usually impossible in a mSUGRA context, where the LSP is considerably lighter than the lighter chargino, but in a more general context may well be possible. If *e.g.* $M_1 = M_2$, it is always possible to find regions in the SUSY parameter space where the sneutrino width becomes very small and L violation may be directly visible.

The signal final state is

$$\ell^- \ell^- \chi^+ \chi^+ + \cancel{E} \quad , \quad \chi^+ \rightarrow f \bar{f}' + \cancel{E} \quad (9)$$

(or the charge conjugated), where $f \bar{f}'$ may be a quark-antiquark pair (*e.g.* $u \bar{d}$), or a lepton pair (*e.g.* $e^+ \nu_e$). To a small fraction the charginos decay into gluinos, which themselves decay into the LSP and two quarks. A possible source for SM background to this signal may

be $t\bar{t}$ -pair production and its subsequent decays, as for example

$$t \rightarrow W^+ b, \quad W^+ \rightarrow \ell^+ \nu_\ell, \quad \bar{b} \rightarrow \bar{c} \ell^+ \nu_\ell$$

However, the ℓ^+ -pair is back-to-back in the center of mass frame of the initial electron-positron beam, whereas the signal- ℓ^+ pair is one-sided (as long as the velocity of the sneutrino does not become too small) and therefore easily discernable. Furthermore, the branching fraction of the b to c decay channel is CKM-suppressed. The same argument holds for any SUSY background sources. Therefore it may be concluded, that the wrong sign lepton signal should be virtually background-free.

III. THE REACTION $e^+ \gamma \rightarrow \tilde{\nu}_\ell^N \tilde{\ell}^+ \bar{\nu}_e$, ($\ell = \mu, \tau$)

In electron-photon collisions μ - and τ -sneutrinos are necessarily produced by graphs at least of order three in perturbation theory. The dominant contributions to higher generation sneutrino production at an electron-photon collider are the ones depicted in Fig. 2, which, as mentioned above, are the leptonic SUSY equivalents to single top-quark production in the SM at an electron-photon facility [14] (the conventions adopted in this section follow closely those of [14]). For the production of first generation slepton pairs additional contributions have to be taken into account, replacing for example in Fig. 2-III the W -boson by a chargino and interchange the sneutrino and the neutrino, and similarly for the remaining contributions. The relevant SUSY interaction Lagrangian are [1]:

$$\begin{aligned} \mathcal{L}_{W\tilde{\nu}\tilde{\ell}} &= \frac{-ig}{\sqrt{2}} W_\mu^+ (\tilde{\nu}_{\ell,L}^* \overleftrightarrow{\partial}^\mu \tilde{\ell}_L) + h.c. , \\ \mathcal{L}_{\gamma\tilde{\ell}\tilde{\ell}} &= ie A_\mu \tilde{\ell}_{L,R}^* \overleftrightarrow{\partial}^\mu \tilde{\ell}_{L,R} , \\ \mathcal{L}_{\gamma W\tilde{\ell}\tilde{\nu}} &= \frac{g}{\sqrt{2}} e A^\mu \tilde{\ell}_L^* \tilde{\nu}_{\ell,L} W_\mu^+ + h.c. . \end{aligned} \tag{10}$$

The gauge invariant amplitude consists of four terms and can be written as

$$\mathcal{M} = \frac{ieg^2}{2} \sum_{i=I}^{IV} T_\mu^i \epsilon^\mu(p_g) . \tag{11}$$

The various contributions are listed in Appendix C.

Here it is not possible to factorize the phase space integral into two two-particle integrations as it was done in the previous section so that the phase space integration is performed numerically using the VEGAS [24] code. Following [25], in the frame $\vec{\mathbf{p}}_{\bar{\nu}} = -\vec{\mathbf{p}}_{\bar{\ell}}$ the total cross-section is given by

$$\sigma_{tot}(s) = \frac{1}{1024\pi^4} \int_{(m_{\bar{\nu}_\ell^N} + m_{\bar{\ell}})^2}^s ds_2 \int_{-(s-s_2)}^0 dt_1 \int d\cos\theta d\phi \frac{\lambda^{1/2}(s_2, m_{\bar{\nu}_\ell^N}^2, m_{\bar{\ell}}^2)}{s_2} |\mathcal{M}|^2, \quad (12)$$

where $s_2 = (p_{\bar{\ell}} + p_{\bar{\nu}_\ell^N})^2$ and $t_1 = (p_e - p_\nu)^2$. The explicit parameterization of the individual four-vectors in terms of the invariants s_2, t_1 and the polar angles of $\vec{\mathbf{p}}_{\bar{\ell}}$ is given in appendix D.

However the $e\gamma$ option of a LC will be realized producing high energy photons through Compton-backscattering of a low energy laser beam with an high energy positron beam [13]. Thus the resulting photons are not monochromatic and one has to fold the cross section of any $e\gamma$ process over a photon energy spectrum. It is expected that a photon collider will operate at luminosities very close to that of the e^+e^- machine. In terms of the variables

$$x = \frac{4E_{e^+}E_{Laser}}{m_e^2} \leq 2(1 + \sqrt{2}) \quad , \quad y = \frac{E_\gamma}{E_{e^+}}$$

the photon energy spectrum is given by [26]

$$\mathcal{P}(y) = \frac{1}{N} \left[1 - y + \frac{1}{1-y} - \frac{4y}{x(1-y)} + \frac{4y^2}{x^2(1-y)^2} \right]. \quad (13)$$

Here the factor

$$N = \frac{1}{2} + \frac{8}{1+x} + \frac{7}{2x(1+x)} + \frac{1}{2x(1+x)^2} + \left(1 - \frac{4}{x} - \frac{8}{x^2}\right) \ln(1+x)$$

normalizes $\int \mathcal{P}(y) dy$ to unity. The resulting cross-section applying eq. (13) is

$$\sigma = \int_{(m_{\bar{\nu}_\ell^N} + m_{\bar{\ell}})^2/s}^{x(x+1)} \mathcal{P}(y) \sigma_{tot}(ys) dy. \quad (14)$$

where σ_{tot} is defined in eq. (12). Assuming the mSUGRA relations for the slepton masses [27]

$$m_{\tilde{\nu}_L}^2 = M_0^2 + 0.07m_g^2 + \frac{1}{2}\cos 2\beta M_Z^2$$

$$m_{\tilde{\ell}_L}^2 = M_0^2 + 0.07m_g^2 + \frac{1}{2}\cos 2\beta M_Z^2(2\sin^2 \Theta_W - 1)$$

The cross-section eq. (12) is plotted in Fig. 7 for the parameters defined in tab. I and for two different values of the center-of-mass energy of the e^+e^- -pair (x was set to its maximum). The cross-section is of order $\mathcal{O}(0.1 \text{ fb})$ at $\sqrt{s}=800 \text{ GeV}$ and M_0 masses of order $\mathcal{O}(100 \text{ GeV})$. For a more realistic center of mass energy of 500 GeV the resulting cross-sections are about an order of magnitude smaller. With luminosities as those projected for a LC of several $10^{34} \text{ cm}^{-2}\text{s}^{-1}$ one produces several tens of single sneutrino events per year.

The process $e^+\gamma \rightarrow \tilde{\nu}_\ell^N \tilde{\ell}^+ \bar{\nu}_e$, ($\ell = \mu, \tau$) can also be exploited at e^+e^- colliders. Here in fact by taking the photon to be virtual the diagrams of Fig. 2 can be attached to the electron current thus describing slepton associated single sneutrino production at e^+e^- colliders. The full process involving virtual photons (with possibly other diagrams) due to the fact that the photon is massless (its propagator gives a factor Q^{-4} in the squared amplitude if Q is the virtual photon momentum) is dominated by small values of Q i.e. quasi real photons and the full e^+e^- process is approximated by folding the cross-section of eq. (12) with a photon distribution function $f_\gamma(x)$. This is the so-called equivalent photon (Weizsäcker-Williams) approximation (E.P.A) which, quite generally, for any scattering process involving a charged particle in the initial state that interacts via a virtual photon, consist in approximating the full process by defining a distribution function for the photon in the electron of energy E . The Weizsäcker-Williams spectrum is given by [28]

$$f_\gamma(x) = \frac{\alpha}{\pi} \log\left(\frac{E}{m_e}\right) \frac{1 + (1-x)^2}{x}$$

and $f_\gamma(x)$ is interpreted as the photon distribution of an electron of energy E i.e. the probability that an electron of energy E radiates a quasi-real photon in the forward direction with energy $E_\gamma = xE$. The cross section at the e^+e^- machine is estimated using the following formula:

$$\sigma = \int_{(m_{\tilde{\nu}_\ell^N} + m_{\tilde{\ell}})^2/s}^1 f_\gamma(x) \sigma_{tot}(xs) dx . \quad (15)$$

Some examples of the results employing eq. (15) for the production of second and third generation single sneutrinos are shown in Fig. 7. Again, for plausible values of slepton masses and center-of-mass energies the resulting total cross-sections are of the order of $\mathcal{O}(0.1 fb)$. Therefore, as in the production of first generation sneutrinos (see ref. [29]) the production of second and third generation sneutrinos at an e^+e^- collider through the $e\gamma$ subprocess appears to be at observable rates provided that the LC will operate at the prospected luminosities of several $10^{34} \text{ cm}^{-2} \text{ s}^{-1}$.

Applying the procedure of the previous section, it is possible to estimate the rate of wrong charged lepton events coming from L-violating sneutrino decays. The resulting cross section for different combinations of parameters is plotted in Fig. 8. In the examples chosen, for a moderate ratio $\Delta m/\overline{m} \approx 10^{-2}$ the L-violating signal may be observable only if both sleptons and charginos are light ($M_0 \approx M_2 \approx |\mu| \approx 100 \text{ GeV}$). For higher masses an appreciable signal is reached only for a large amount of L-violation.

Note that in mSUGRA the $SU(2)_L$ -doublet charged sleptons are slightly heavier than the $SU(2)_L$ -doublet sneutrinos. This fact renders the process discussed here less favourable than the process discussed in the previous section. Larger cross-sections for single μ - and τ -sneutrino production may be possible in scenarios where charged sleptons are allowed to be (considerably) lighter than the sneutrinos. Two examples shown in Fig. 9 illustrate this fact. For the parameters chosen, L-violating cross sections of order $\mathcal{O}(0.01 \text{ fb})$ can be obtained for $\Delta m/\overline{m} \approx 0.01$ for higher values of \overline{m} in respect to the mSUGRA case in Fig. 8.

As far as the comparison with low-energy limits on Δm are concerned, the same remarks as in the previous section apply.

If the initial state lepton is a positron, the signal final states are (assuming the final state leptons being not too soft)

$$\chi^- \ell^+ \ell^+ + \mathbb{E} \text{ (for } \tilde{\ell}^+ \rightarrow \ell + \chi^0 \text{) , } \chi^- \ell^+ \chi^+ + \mathbb{E} \text{ (for } \tilde{\ell}^+ \rightarrow \chi^+ \tilde{\nu}_\ell \text{) .} \quad (16)$$

The possible chargino decay modes have been mentioned in eq. (9). In the SM the second or third generation ℓ^+ pair may be produced in e - γ -collisions in at least 7th order of perturbation theory in the decay chain of a top-bottom final state (with additional CKM suppression). The rate of such a process is negligible even compared to the very low signal rate. The second signal in eq. (16) may be mimicked by the production of a Z^0 - e^+ pair (the Z^0 decaying into ℓ 's), when the charginos to a large fraction decay into the $\ell^+\nu_\ell\chi^0$ final state. The same reasoning holds for the SUSY background: *e.g.* the final state containing two charginos may be reproduced by the decays of a selectron and a non-LSP neutralino

$$e^+\gamma \rightarrow \tilde{e}^+\chi^0, \tilde{e}^+ \rightarrow \chi^+\bar{\nu}_e, \chi^0 \rightarrow \chi^-\ell^+\nu_\ell.$$

If the $\tilde{\ell}$ decays to a large fraction directly into the LSP (thus producing a $\ell^+\ell^+$ final state) the background may be eliminated discarding events with only one ℓ^+ in the final state. In the opposite case, a detailed analysis of the angular and energy distribution of the final state particles is required.

IV. CONCLUSIONS

In conclusion, L violation in the sneutrino sector of supersymmetric extensions of the Standard Model may manifest itself by producing the wrong charged lepton signal by decays of sneutrinos into charginos and charged leptons. If the average of the two sneutrino mass states is large, sneutrino pair production is excluded and associated single sneutrino production has to be considered in future collider facilities such as the NLC or an electron-photon machine.

For chargino-associated single sneutrino production at the NLC, under favourable circumstances (large branching fraction of the chargino-lepton decay channel and a relative low average sneutrino mass) one may expect about ten wrong sign lepton events per year for a relative mass-splitting $\Delta m/\overline{m} \approx 0.01$ and for widths of the sneutrino mass states of order $\mathcal{O}(1 \text{ GeV})$. Such an amount of L violation is compatible with a neutrino mass of order

$\mathcal{O}(10 \text{ keV})$ and thus with the kinematical limits on second and third generation neutrino, but not compatible with the limit on the left-handed neutrino Majorana mass matrix from the neutrinoless double beta decay combined with the oscillation solution to the solar and atmospheric neutrino problems.

Since the signal is virtually background-free, the number of expected wrong sign lepton events should be sufficient to detect L violation in the sneutrino sector. However, under unfavourable circumstances less than one wrong charge lepton event per year is expected. Then an appreciable event rate is possible only for a relative sneutrino mass-splitting near to one.

For charged slepton associated sneutrino production at an electron photon collider, in mSUGRA models the event rate of the wrong charged lepton signal is very low for realistic slepton masses and a relative sneutrino mass-splitting of order 0.01. In order to produce a detectable event rate the relative mass-splitting must be close to one. If the charged slepton is considerably lighter than the average sneutrino mass, an observable event rate is possible for moderate values of the mass-splitting.

ACKNOWLEDGMENTS

O. P. would like to thank the Max-Planck-Institut für Kernphysik, for the very warm hospitality during his stay in Heidelberg.

APPENDIX A: CONTRIBUTIONS TO $e^+e^- \rightarrow \chi^\pm \tilde{\nu}_\ell^N \ell^\mp$, $\ell = \mu, \tau$

In the following individual contributions to the cross section for the reaction $e^+e^- \rightarrow \chi^\pm \tilde{\nu}_\ell^N \ell^\mp$ (Fig. 1) are listed for $\ell = \mu, \tau$. For $\ell = e$ further contributions have to be taken into account. The contribution of the Higgs exchange diagram has been neglected since it is proportional to the electron mass. The index i corresponds to the final state chargino (for obtaining numerical results only production of the lighter chargino was considered), the indices j, j' correspond to exchanged charginos. V, V' stands for either γ or Z^0 and N is the index for the heavier ($N=1$) or lighter ($N=2$) sneutrino mass states. m_D is the usual L -conserving sneutrino mass. The modification of the sneutrino propagator in the presence of L violation has been neglected. Propagator factors $1/[(M^2 - X)^2 + M^2 \Gamma_M^2]$ are denoted by $P(M, X)$. The integration limits of $Q^2 = (p_{\tilde{\nu}_\ell^N} + p_\ell)^2$ are

$$Q_{max,min}^2 = (\sqrt{s} - m_i)^2, (m_\ell + m_{\tilde{\nu}_\ell^N})^2$$

unless noted otherwise. The total cross section is a sum of the contributions depicted in Fig. 1 and their interferences. The interference between 1-III and the other graphs is neglected since in the numerical examples displayed in tab. I the contribution of 1-III is much smaller than the contribution from both 1-I and 1-II.

The contribution from (t -channel) sneutrino-exchange shown in Fig. 1-I is defined as

$$\begin{aligned} \sigma_i^{(I,I)} &= \frac{1}{2s} \frac{1}{4} \sum_{j,j'} g^6 |V_i|^2 |V_j|^2 |V_{j'}|^2 \frac{1}{128\pi^3} \int dQ^2 \lambda^{1/2}(1, \frac{m_\ell^2}{Q^2}, \frac{m_{\tilde{\nu}_\ell^N}^2}{Q^2}) P(m_j, Q^2) \\ &\times P(m_{j'}, Q^2) (Q^2 + m_\ell^2 - m_{\tilde{\nu}_\ell^N}^2) ((m_j^2 - Q^2)(m_{j'}^2 - Q^2) + m_j m_{j'} \Gamma_j \Gamma_{j'}) \\ &\times \left[\lambda^{1/2}\left(\frac{Q^2}{s}, \frac{m_i^2}{s}, 1\right) \left(1 + \frac{(Q^2 - m_{\tilde{\nu}_\ell^N}^2)(m_i^2 - m_{\tilde{\nu}_\ell^N}^2)}{(Q^2 - m_{\tilde{\nu}_\ell^N}^2)(m_i^2 - m_{\tilde{\nu}_\ell^N}^2) + m_{\tilde{\nu}_\ell^N}^2 s}\right) \right. \\ &\left. + \frac{1}{s} (2m_{\tilde{\nu}_\ell^N}^2 - m_i^2 - Q^2) \ln F(Q^2) \right], \end{aligned}$$

where as usual $\lambda(a, b, c) = a^2 + b^2 + c^2 + 2ab + 2ac + 2bc$ and the function $F(Q^2)$ is defined as

$$F(Q^2) = (m_i^2 - \tilde{m}_D^2 + \frac{1}{2}(Q^2 - m_i^2 - s) + \frac{1}{2}\lambda^{1/2}(Q^2, m_i^2, s)) \\ \times (m_i^2 - \tilde{m}_D^2 + \frac{1}{2}(Q^2 - m_i^2 - s) - \frac{1}{2}\lambda^{1/2}(Q^2, m_i^2, s))^{-1} .$$

The contribution from (s -channel) gauge-boson-exchange depicted in Fig. 1-II is defined as

$$\sigma_i^{(\text{II}, \text{II})} = \frac{1}{2s} \frac{1}{4} \sum_{j, j'} \sum_{V, V'} g^2 V_{j1} V_{j'1} (g_V^L g_{V'}^L + g_V^R g_{V'}^R) \frac{1}{32\pi^3} \int dQ^2 \lambda^{1/2}(1, \frac{m_\ell^2}{Q^2}, \frac{m_{\tilde{\nu}_\ell^N}^2}{Q^2}) \\ \times (Q^2 + m_\ell^2 - m_{\tilde{\nu}_\ell^N}^2) \lambda^{1/2}(1, \frac{m_l^2}{s}, \frac{Q^2}{s}) P(V, s) P(V', s) P(j, Q^2) P(j', Q^2) \\ \times G(Q^2) \left\{ \frac{1}{3} s^2 \left[\lambda(1, \frac{m_i^2}{s}, \frac{Q^2}{s}) + (1 + \frac{m_i^2}{s} + \frac{Q^2}{s} - \frac{2(m_i^2 - Q^2)^2}{s^2}) \right] \right. \\ \times \left[Q^2 (O'_{ji})_V (O'_{ji})^* + m_j m_{j'} (O'_{ji})_V (O'_{ji})_{V'}^* \right] \\ \left. + 2Q^2 s \left[m_{j'} m_i (O'_{ji})_V (O'_{ji})_{V'}^* + m_{j'} m_i (O'_{ji})_V (O'_{ji})_{V'}^* \right] \right\} ,$$

where the function $G(Q^2)$ is given by

$$G(Q^2) = \left[(m_V^2 - s) \{ (m_{V'}^2 - s) a - m_{V'} \Gamma_{V'} b \} \right. \\ \left. + m_V \Gamma_V \{ m_{V'} \Gamma_{V'} a + (m_{V'}^2 - s) b \} \right] ; \\ a = (m_j^2 - Q^2)(m_{j'}^2 - Q^2) + m_j m_{j'} \Gamma_j \Gamma_{j'} \\ b = m_{j'} \Gamma_{j'} (m_j^2 - Q^2) - m_j \Gamma_j (m_{j'}^2 - Q^2) .$$

The lepton-gauge boson couplings $g_V^{L,R}$ are

$$g_{Z^0}^L = \frac{g}{\cos \Theta_W} \left(\frac{1}{2} - \sin^2 \Theta_W \right) , \quad g_{Z^0}^R = \frac{g}{\cos \Theta_W} (-\sin^2 \Theta_W)$$

$$g_\gamma^L = g_\gamma^R = e ,$$

and the gauge boson-chargino couplings $(O'_{ij})_V^{L,R}$ are

$$(O'_{ij})_{Z^0} = \frac{g}{\cos \Theta_W} (-V_{i1} V_{j1}^* - \frac{1}{2} V_{i2} V_{j2}^* + \delta_{ij} \sin^2 \Theta_W)$$

$$(O'_{ij})_{Z^0} = \frac{g}{\cos \Theta_W} (-U_{i1}^* U_{j1} - \frac{1}{2} U_{i2}^* U_{j2} + \delta_{ij} \sin^2 \Theta_W)$$

$$(O'_{ij})_\gamma = (O'_{ij})_\gamma = -e \delta_{ij}$$

(Note that $(O'_{ij})_{Z^0} = (O'_{ji})_{Z^0}^*$).

The interference between sneutrino and gauge boson graphs is

$$\begin{aligned} \sigma_i^{(I,II)} &= \frac{1}{2s} \frac{1}{4} \sum_{j,j'} g^4 |V_{i1}|^2 |V_{j1}|^2 \frac{1}{32\pi^3} \int dQ^2 (Q^2 + m_\ell^2 - m_{\tilde{\nu}_\ell^N}^2) \lambda^{1/2} \left(1, \frac{m_\ell^2}{s}, \frac{Q^2}{s}\right) \\ &\times P(j, Q^2) P(j', Q^2) P(V, s) \left\{ (m_V^2 - s) [(m_j^2 - Q^2)(m_{j'}^2 - Q^2) + m_j m_{j'} \Gamma_j \Gamma_{j'}] \right. \\ &\quad \left. - m_V \Gamma_V [(m_j^2 - Q^2) m_{j'} \Gamma_{j'} - (m_{j'}^2 - Q^2) m_j \Gamma_j] \right\} \\ &\times \left\{ m_i m_{j'} (O'_{ij'})_V^* (-\ln F(Q^2)) + \frac{1}{2} (O'_{ij'})_V^* \left[\lambda^{1/2} \left(\frac{Q^2}{s}, \frac{m_i^2}{s}, 1 \right) \right. \right. \\ &\quad \left. \left. \times \left(\frac{1}{2} (Q^2 + m_i^2 - s) - \tilde{m}_D^2 \right) - \frac{1}{s} (Q^2 - \tilde{m}_D^2) (m_i^2 - \tilde{m}_D^2) \ln F(Q^2) \right] \right\} \end{aligned}$$

and the function $F(Q^2)$ has been defined above.

The contribution from the double sneutrino graph is

$$\begin{aligned} \sigma_i^{(III,III)} &= \frac{1}{2s} \frac{1}{4} \frac{1}{(2\pi)^5} \frac{1}{8} |V_{i1}|^2 \frac{g^6}{c_W^2} \frac{\pi^2}{3} s^2 \int dQ^2 P(m_{Z^0}, s) P(m_{\tilde{\nu}_\ell^N}, Q^2) \\ &\times \lambda^{1/2} \left(1, \frac{Q^2}{s}, \frac{m_{\tilde{\nu}_\ell^N}^2}{s}\right) \lambda^{1/2} \left(1, \frac{m_\ell^2}{Q^2}, \frac{m_{\chi_i}^2}{Q^2}\right) (Q^2 - m_{\chi_i}^2 - m_\ell^2) \\ &\times \left[1 - 2 \frac{m_{\tilde{\nu}_\ell^N}^2}{s} - 2 \frac{Q^2}{s} - \frac{1}{2} \lambda \left(1, \frac{Q^2}{s}, \frac{m_{\tilde{\nu}_\ell^N}^2}{s}\right) + \frac{(m_{\tilde{\nu}_\ell^N}^2 - Q^2)^2}{s^2} \right]. \end{aligned}$$

The integration limits are $Q_{min}^2 = (m_\ell + m_{\chi_i})^2$ and $Q_{max}^2 = (\sqrt{s} - m_{\tilde{\nu}_\ell^N})^2$. Note that $N \neq N'$ due to the off-diagonality of the $Z^0 \tilde{\nu}_\ell^1 \tilde{\nu}_\ell^2$ vertex.

APPENDIX B: CONTRIBUTIONS TO $e^+\gamma \rightarrow \tilde{\nu}_\ell^N \tilde{\ell}^+ \bar{\nu}_e$, $\ell = \mu, \tau$

The individual amplitudes of the graphs shown in Fig. 2 are given by

$$\begin{aligned}
T_\mu^{(I)} &= -D(s_2)D(t_1)j^\alpha(p_-)_\beta(g^{\beta\nu} - \frac{Q^\beta Q^\nu}{m_W^2})S_{\mu\nu\alpha} , \\
T_\mu^{(II)} &= D(s_2)(p_-)_\alpha(g^{\alpha\nu} - \frac{Q^\alpha Q^\nu}{m_W^2})\bar{v}(p_e)\gamma_\mu \frac{-(\not{p}_g + \not{p}_e)}{s}\gamma_\nu P_L v(p_\nu) , \\
T_\mu^{(III)} &= -D(t_1)j_\mu , \\
T_\mu^{(IV)} &= D(t_1)\frac{1}{m_\ell^2 - K^2}j^\alpha[K_\mu K_\alpha + (p_{\tilde{\nu}_\ell^N})_\alpha(K - p_{\tilde{l}})_\mu - (p_{\tilde{l}})_\mu K_\alpha] .
\end{aligned}$$

The sum of the first and the third contribution can be simplified to give

$$\begin{aligned}
(T^{(I)} + T^{(III)})_\mu &= D(s_2)D(t_1)j^\alpha p_-^\beta 2(g_{\alpha\beta}P_\mu + g_{\mu\alpha}(p_g)_\beta - g_{\mu\beta}(p_g)_\alpha) \\
&\quad + D(s_2)\frac{-1}{s}p_-^\alpha \bar{v}(p_e)\gamma_\mu(\not{p}_g + \not{p}_e)\gamma_\alpha P_L v(p_\nu) .
\end{aligned}$$

Here we have defined

$$\begin{aligned}
p_- &= p_{\tilde{l}} - p_{\tilde{\nu}_\ell^N}, \quad K = p_g - p_{\tilde{l}}, \quad Q = p_{\tilde{l}} + p_{\tilde{\nu}_\ell^N}, \quad P = p_e - p_\nu, \quad t_1 = P^2, \quad s_2 = Q^2, \\
j^\alpha &= \bar{v}(p_e)\gamma^\alpha P_L v(p_\nu), \quad S_{\mu\nu\alpha} = -g_{\alpha\nu}(P + Q)_\mu + g_{\mu\alpha}(P - p_g)_\nu + g_{\mu\nu}(Q + p_g)_\alpha, \\
D(s_2) &= (m_W^2 - s_2 + i\Gamma_W m_W)^{-1}, \quad D(t_1) = (m_W^2 - t_1)^{-1} .
\end{aligned}$$

Replacing in [14] the quark charges e_t, e_b by 0, 1 respectively and the quark current J_{quark}^μ by $p_-^\mu = p_{\tilde{l}} - p_{\tilde{\nu}_\ell^N}$ (stemming from the derivative $W\tilde{\ell}\tilde{\nu}_\ell$ coupling) leads to the equivalent expressions of the amplitudes $T_\lambda^{(III)}, T_\lambda^{(IV)}$ in [14]. A subtlety known from scalar electrodynamics arises in the calculation of the time ordered product of the propagators of the exchanged scalar fields. Here the additional contribution from taking the partial derivatives out of the time ordered product is cancelled by the $W\gamma\tilde{\nu}_\ell\tilde{\ell}$ four point vertex.

APPENDIX C: FOUR-VECTOR PARAMETRIZATION IN TERMS OF TWO INVARIANTS AND TWO ANGLES

In order to carry out the numerical phase space integration in the process $e\gamma \rightarrow \tilde{\ell}^+ \tilde{\nu}_\ell^N \bar{\nu}_e$ following [25] the four-vectors in the process can be parametrized in terms of two invariants (see appendix C) and one solid angle as

$$p_\gamma = \begin{pmatrix} \frac{s-s_2}{2\sqrt{s_2}} \left[\sin^2 \Theta + \left(\cos \Theta + \frac{s_2-t_1}{s-s_2} \right)^2 \right]^{1/2} \\ \sin \Theta \frac{s-s_2}{2\sqrt{s_2}} \\ 0 \\ \frac{s-s_2}{2\sqrt{s_2}} \left[\cos \Theta \frac{s_2-t_1}{s-s_2} \right] \end{pmatrix}, \quad p_e = \begin{pmatrix} \frac{s_2-t_1}{2\sqrt{s}} \\ 0 \\ 0 \\ \frac{s_2-t_1}{2\sqrt{s}} \end{pmatrix},$$

$$p_\nu = \begin{pmatrix} \frac{s-s_2}{2\sqrt{s_2}} \\ \sin \Theta \frac{s-s_2}{2\sqrt{s_2}} \\ 0 \\ \cos \Theta \frac{s-s_2}{2\sqrt{s_2}} \end{pmatrix}, \quad p_{\tilde{\ell}} = \begin{pmatrix} \left[m_{\tilde{\ell}}^2 + \frac{\lambda(s_2, m_{\tilde{\nu}_\ell^N}^2, m_{\tilde{\ell}}^2)}{4s_2} \right]^{1/2} \\ \frac{\lambda(s_2, m_{\tilde{\nu}_\ell^N}^2, m_{\tilde{\ell}}^2)^{1/2}}{2\sqrt{s_2}} \sin \theta \cos \phi \\ \frac{\lambda(s_2, m_{\tilde{\nu}_\ell^N}^2, m_{\tilde{\ell}}^2)^{1/2}}{2\sqrt{s_2}} \sin \theta \sin \phi \\ \frac{\lambda(s_2, m_{\tilde{\nu}_\ell^N}^2, m_{\tilde{\ell}}^2)^{1/2}}{2\sqrt{s_2}} \cos \theta \end{pmatrix}$$

$$p_{\tilde{\nu}_\ell^N} = \begin{pmatrix} \left[m_{\tilde{\nu}_\ell^N}^2 + \frac{\lambda(s_2, m_{\tilde{\nu}_\ell^N}^2, m_{\tilde{\ell}}^2)}{4s_2} \right]^{1/2} \\ -\vec{\mathbf{p}}_3 \end{pmatrix},$$

$$\cos \Theta = \frac{(s-s_2)(s_2-t_1) - 2s_2(s-s_2-t_1)}{(s_2-t_1)(s-s_2)}.$$

REFERENCES

- [1] H.E. Haber and G.L. Kane, Phys. Rep. 117 (1985) 76.
- [2] M. Hirsch, H.V. Klapdor-Kleingrothaus and S. Kovalenko, Phys. Lett. B 398 (1997) 311.
- [3] Y. Grossmann and H.E. Haber, Phys. Rev. Lett. 78 (1997) 3438.
- [4] M. Hirsch, H.V. Klapdor-Kleingrothaus and S. Kovalenko, Phys. Lett. B 403 (1997) 291.
- [5] M. Hirsch, H.V. Klapdor-Kleingrothaus and S. Kovalenko, Phys. Rev. D 57 (1998) 1947.
- [6] H.V. Klapdor-Kleingrothaus, St. Kolb and V.A. Kuzmin, Phys. Rev. D 62 (2000) 035014.
- [7] M. Hirsch, H.V. Klapdor-Kleingrothaus, St. Kolb and S. Kovalenko, Phys. Rev D 57 (1998) 2020.
- [8] L.J. Hall, T. Moroi and H. Murayama, Phys. Lett. B 424 (1998) 305.
- [9] St. Kolb, M. Hirsch, H.V. Klapdor-Kleingrothaus and O. Panella, Phys. Lett. B 478 (2000) 262.
- [10] L.E. Ibáñez, Phys. Lett. B 137 (1984) 160; J.S. Hagelin, G.L. Kane and S. Raby, Nucl. Phys. B 241 (1984) 638.
- [11] T. Falk, K.A. Olive and M. Srednicki Phys. Lett. B 339 (1994) 248.
- [12] H. Murayama and M.E. Peskin, Ann. Rev. Nucl. Part. Sci. 46 (1996) 533.
- [13] I. Ginzburg, G. Kotin, V. Serbo and V. Telnov, Nucl. Instrum. and Meth. 205 (1983) 47; I. Ginzburg, G. Kotin, S. Panfil, V. Serbo and V. Telnov, Nucl. Instrum. and Meth. 219 (1984) 5.
- [14] O. Panella, G. Pancheri and Y.N. Srivastava, Phys. Lett. B 318 (1993) 241.

- [15] A. Wagner, Nucl. Phys. B (Proc. Suppl.) **79**, (1999) 643-651. Cern Courier, 40 2000, No.5, 19-20.
- [16] V. Telnov, Int. J. Mod. Phys. A 15, 2577-2586 (2000).
- [17] Y. Grossman and H.E. Haber, Phys. Rev. D 59 (1999) 093008; Y. Grossman and H.E. Haber, E-print archive hep-ph/0005276.
- [18] T. Wöhrmann and H. Fraas, Phys. Rev. D 52 (1995) 78.
- [19] V. Barger and R. Phillips, “Collider Physics” (Addison-Wesley, Redwood City, CA, 1987).
- [20] D.E. Groom *et al.*, Europ. Phys. J. C 15 (2000) 1.
- [21] L. Baudis *et al.*, Phys. Rev. Lett. 83 (1999) 41.
- [22] See talks at Neutrino 2000,
<http://ALUMNI.LAURENTIAN.CA/www/physics/nu2000/>
- [23] G. Bhattacharyya, H.V. Klapdor-Kleingrothaus and H. Päs, Phys. Lett. B 463 (1999) 77.
- [24] G. P. Lepage, J. Comput. Phys. **27**, 192 (1978).
- [25] E. Byckling and K. Kajantie, “Particle Kinematics” (John Wiley, 1973).
- [26] A. Ghosal, A. Kundu and B. Mukhopadhyaya, Phys. Rev. D 57 (1998) 1972.
- [27] J. Ellis, G.L. Fogli and E. Lisi, Nucl. Phys. B 393 (1993) 3.
- [28] E. Fermi, Z. Phys. 29 (1924) 315; C. Weiszäcker and E. Williams, Z. Phys. 88 (1934) 612; H. Terazawa, Rev. Mod. Phys. 45 (1973) 615; P. Kessler, Acta Physica Austriaca, 41 (1975) 141-188.
- [29] S. Hesselbach and H. Fraas, Phys. Rev. D 55 (1997) 1343.

FIGURES

FIG. 1. Contributions to $e^+e^- \rightarrow \tilde{\nu}_l^N \ell^- \tilde{\chi}_i^+$ where $N=1,2$ and $\ell=\mu, \tau$ (for $\ell=e$ more graphs contribute)

FIG. 2. Contributions to $e^+\gamma \rightarrow \tilde{\nu}_\ell^N \tilde{\ell}^+ \bar{\nu}_e$. These are the leptonic analogs to single top production in the SM. Graph II containing a four point vertex has no SM-counterpart.

FIG. 3. Cross-section for chargino-associated sneutrino production depicted in Fig. 1-I and 1-II as a function of the sneutrino mass. The curves correspond to the parameters ($\sqrt{s}=500$ GeV; parameter set A; lower solid line); ($\sqrt{s}=800$ GeV; set A; upper solid line); ($\sqrt{s}=500$ GeV; set B; lower dashed line); ($\sqrt{s}=800$ GeV; set A; upper dashed line). The parameter sets A and B have been defined in tab. I. The sneutrino has been taken to be heavier than the charginos, otherwise the production of two real charginos is allowed and the chargino width must be taken into account.

FIG. 4. The L-violating parameter ξ defined in eq. (6) as a function of the dimensionless ratio $\Delta m/\bar{m}$. The various curves refer to the parameters used in Fig. 3 with the same notation.

FIG. 5. Cross-section for the wrong sign charged lepton signal stemming from the chargino-associated sneutrino production depicted in Fig. 1-I and 1-II as a function of the ratio $\Delta m/\bar{m}$. The curves correspond to the parameters $\sqrt{s}=500$ GeV, $\bar{m}=275$ GeV (parameter set A, upper solid line); $\sqrt{s}=500$ GeV, $\bar{m}=350$ GeV (set A, lower solid line); $\sqrt{s}=800$ GeV, $\bar{m}=450$ GeV (set A, upper dashed line); $\sqrt{s}=800$ GeV, $\bar{m}=600$ GeV (set A, lower dashed line); $\sqrt{s}=800$ GeV, $\bar{m}=450$ GeV (set B, upper dotted line); $\sqrt{s}=800$ GeV, $\bar{m}=600$ GeV (set B, lower dotted line). The parameter sets A and B have been defined in tab. I.

FIG. 6. Cross section of the wrong sign lepton signal for the case of a very small common sneutrino width $\Gamma := \Gamma^{tot}(\tilde{\nu}^1) = \Gamma^{tot}(\tilde{\nu}^2) = \Gamma(\tilde{\nu}^1 \rightarrow \chi^\pm \ell^\mp) = \Gamma(\tilde{\nu}^2 \rightarrow \chi^\pm \ell^\mp)$ and for the parameters (set A; $\sqrt{s}=500$ GeV; $\overline{m}=275$ GeV) in dependence of Δm (in GeV). The solid line corresponds to $\Gamma=10$ MeV, the dashed line corresponds to $\Gamma=1$ MeV and the dot-dashed line to $\Gamma=100$ keV. For a neutrino mass of order $\mathcal{O}(1 \text{ eV})$ ($\Delta m \approx 200 \text{ keV} = 2 \times 10^{-4} \text{ GeV}$, see eq. 8) the L-violating signal is of order $\mathcal{O}(0.01 \text{ fb})$ (dashed line).

FIG. 7. Cross-section for $e^+ \gamma \rightarrow \tilde{\nu}_\ell^N \tilde{\ell}^+ \bar{\nu}_e$ in a mSUGRA scenario as a function of the common scalar mass M_0 , applying the backscattering process (B.S.) eq. (14) and the equivalent photon approximation (E.P.A) eq. (15). The curves correspond to the parameters ($\sqrt{s}=800$ GeV, parameter set A; E.P.S.; upper solid line); ($\sqrt{s}=500$ GeV, set A; E.P.S.; lower solid line); ($\sqrt{s}=800$ GeV, set B; E.P.S.; upper long-dashed line); ($\sqrt{s}=500$ GeV, set B; E.P.S.; lower long-dashed line); ($\sqrt{s}=800$ GeV, set A; B.S.; upper dashed line); ($\sqrt{s}=500$ GeV, set A; B.S.; lower dashed line); ($\sqrt{s}=800$ GeV, set B; B.S.; upper dotted line); ($\sqrt{s}=500$ GeV, set B; B.S.; lower dotted line). The parameter sets A and B have been defined in tab. I (the center of mass energy refers to the electron-positron beam).

FIG. 8. Cross-section for the wrong sign charged lepton signal stemming from $e^+ \gamma \rightarrow \tilde{\nu}_\ell^N \tilde{\ell}^+ \bar{\nu}_e$ (in a mSUGRA scenario) as a function of the ratio $\Delta m/\overline{m}$ applying the backscattering process (B.S.) eq. (14) and the equivalent photon approximation (E.P.A) eq. (15). The curves correspond to ($\sqrt{s}=500$ GeV, $M_0=100$ GeV; parameter set A; E.P.S.; upper solid line); ($\sqrt{s}=500$ GeV, $M_0=100$ GeV; set A; B.S.; lower solid line); ($\sqrt{s}=800$ GeV, $M_0=300$ GeV; set A; E.P.S.; upper dashed line); ($\sqrt{s}=800$ GeV, $M_0=300$ GeV; set A; B.S.; lower dashed line); ($\sqrt{s}=800$ GeV, $M_0=300$ GeV; set B; E.P.S.; upper dotted line); ($\sqrt{s}=800$ GeV, $M_0=300$ GeV; set B; B.S.; lower dotted line). The parameter sets A and B have been defined in tab. I. For $M_0=100$ GeV the data is cut off where the lighter sneutrino becomes lighter than the LSP, the bump corresponds to the value of Δm where the heavier sneutrino is not produced any more.

FIG. 9. Cross-section for the wrong sign charged lepton signal stemming from $e^+\gamma \rightarrow \tilde{\nu}_\ell^N \tilde{\ell}^+ \bar{\nu}_e$ as a function of the ratio $\Delta m/\bar{m}$ applying the backscattering process (B.S.) eq. (14). No mSUGRA conditions were assumed. The curves correspond to ($\sqrt{s}=500$ GeV, $\bar{m}=200$ GeV; $m_{\tilde{\ell}}=100$ GeV; parameter set A; B.S.; solid line); ($\sqrt{s}=800$ GeV, $\bar{m}=300$ GeV; $m_{\tilde{\ell}}=200$ GeV; parameter set A; B.S.; dashed line); The parameter set A has been defined in tab. I.

TABLES

TABLE I. Parameters used for numerical results assuming a gravity mediated GUT scheme.

V (N) is the chargino (neutralino) mixing matrix.

Set A: $\mu = -100$ GeV , $M_2 = 100$ GeV , $\tan\beta = 2$			
$m_{\chi_1^+} = 151.1$ GeV	$m_{\chi_2^+} = 100.3$ GeV	$V(1, 1) = 0.89$	$V(1, 2) = -0.44$
$m_{\chi_1^0} = 143.6$ GeV	$m_{\chi_2^0} = 134.5$ GeV	$m_{\chi_3^0} = 86.2$ GeV	$m_{\chi_4^0} = 54.8$ GeV
$N(1, 1) = -0.20$	$N(2, 1) = -0.21$	$N(3, 1) = -0.11$	$N(4, 1) = -0.95$
$N(1, 2) = 0.78$	$N(2, 2) = 0.30$	$N(3, 2) = -0.51$	$N(4, 2) = -0.18$
Set B: $\mu = -200$ GeV , $M_2 = 200$ GeV , $\tan\beta = 35$			
$m_{\chi_1^+} = 263.5$ GeV	$m_{\chi_2^+} = 153.2$ GeV	$V(1, 1) = 0.80$	$V(1, 2) = -0.60$
$m_{\chi_1^0} = 262.2$ GeV	$m_{\chi_2^0} = 211.7$ GeV	$m_{\chi_3^0} = 155.7$ GeV	$m_{\chi_4^0} = 94.3$ GeV
$N(1, 1) = 0.15$	$N(2, 1) = -0.10$	$N(3, 1) = -0.30$	$N(4, 1) = 0.93$
$N(1, 2) = -0.70$	$N(2, 2) = 0.14$	$N(3, 2) = -0.69$	$N(4, 2) = -0.10$

LIST OF FIGURES

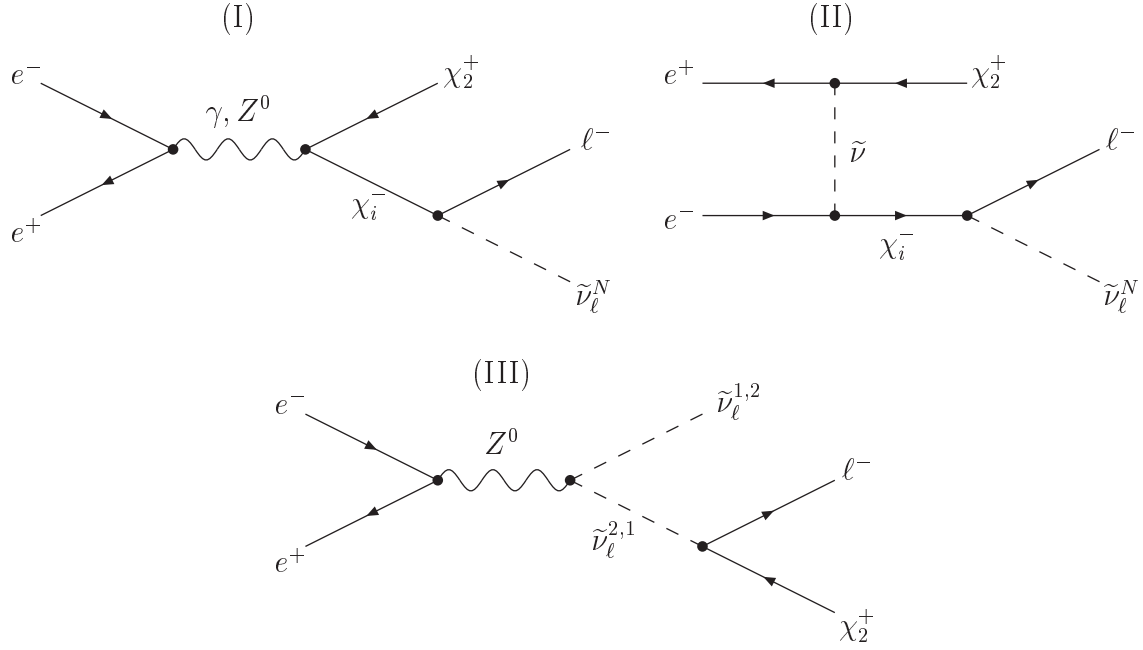


FIG. 1. Contributions to $e^+e^- \rightarrow \tilde{\nu}_\ell^N \ell^- \tilde{\chi}_i^+$ where $N=1,2$ and $\ell=\mu, \tau$ (for $\ell=e$ more graphs contribute)

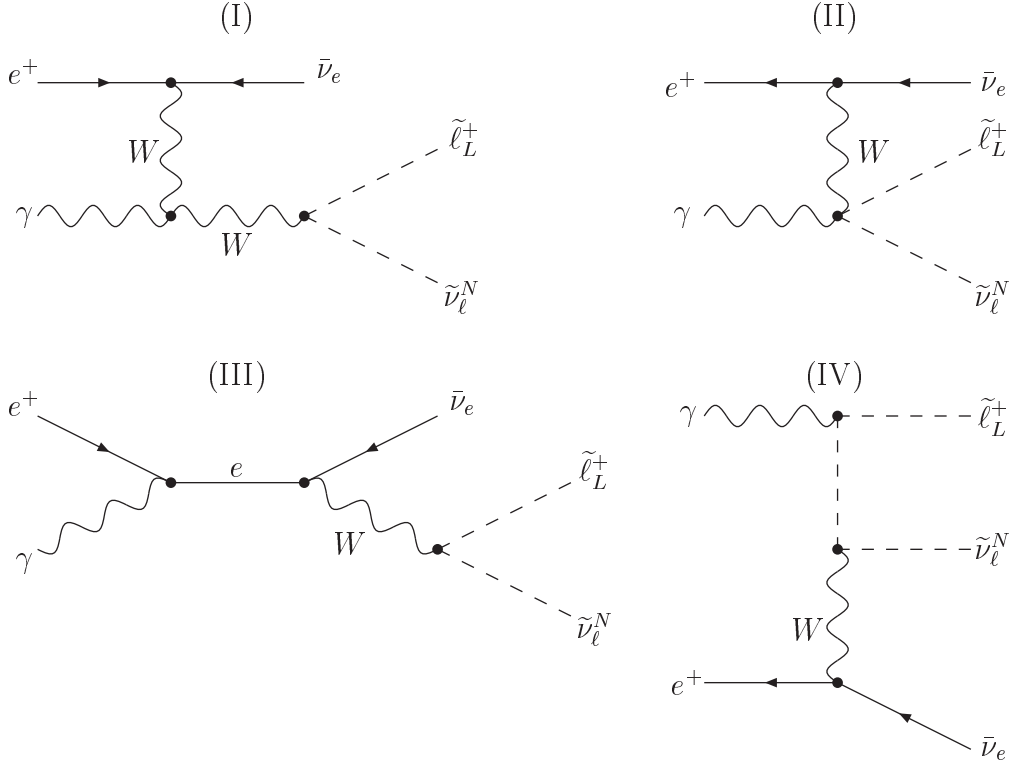


FIG. 2. Contributions to $e^+ \gamma \rightarrow \tilde{\nu}_\ell^N \tilde{\ell}_L^+ \bar{\nu}_e$. These are the leptonic analogs to single top production in the SM. Graph II containing a four point vertex has no SM-counterpart.

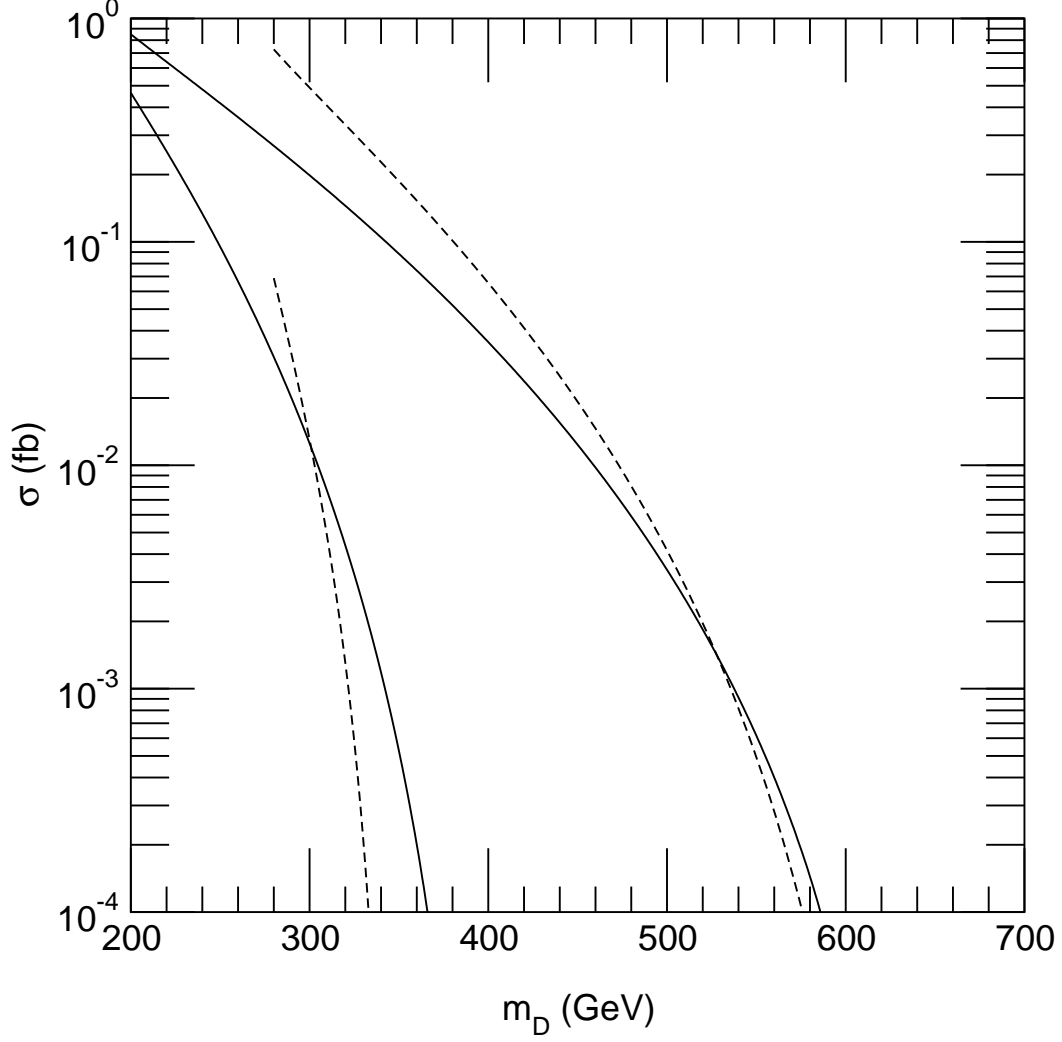


FIG. 3. Cross-section for chargino-associated sneutrino production depicted in Fig. 1-I and 1-II as a function of the sneutrino mass. The curves correspond to the parameters ($\sqrt{s}=500$ GeV; parameter set A; lower solid line); ($\sqrt{s}=800$ GeV; set A; upper solid line); ($\sqrt{s}=500$ GeV; set B; lower dashed line); ($\sqrt{s}=800$ GeV; set A; upper dashed line). The parameter sets A and B have been defined in tab. I. The sneutrino has been taken to be heavier than the charginos, otherwise the production of two real charginos is allowed and the chargino width must be taken into account.

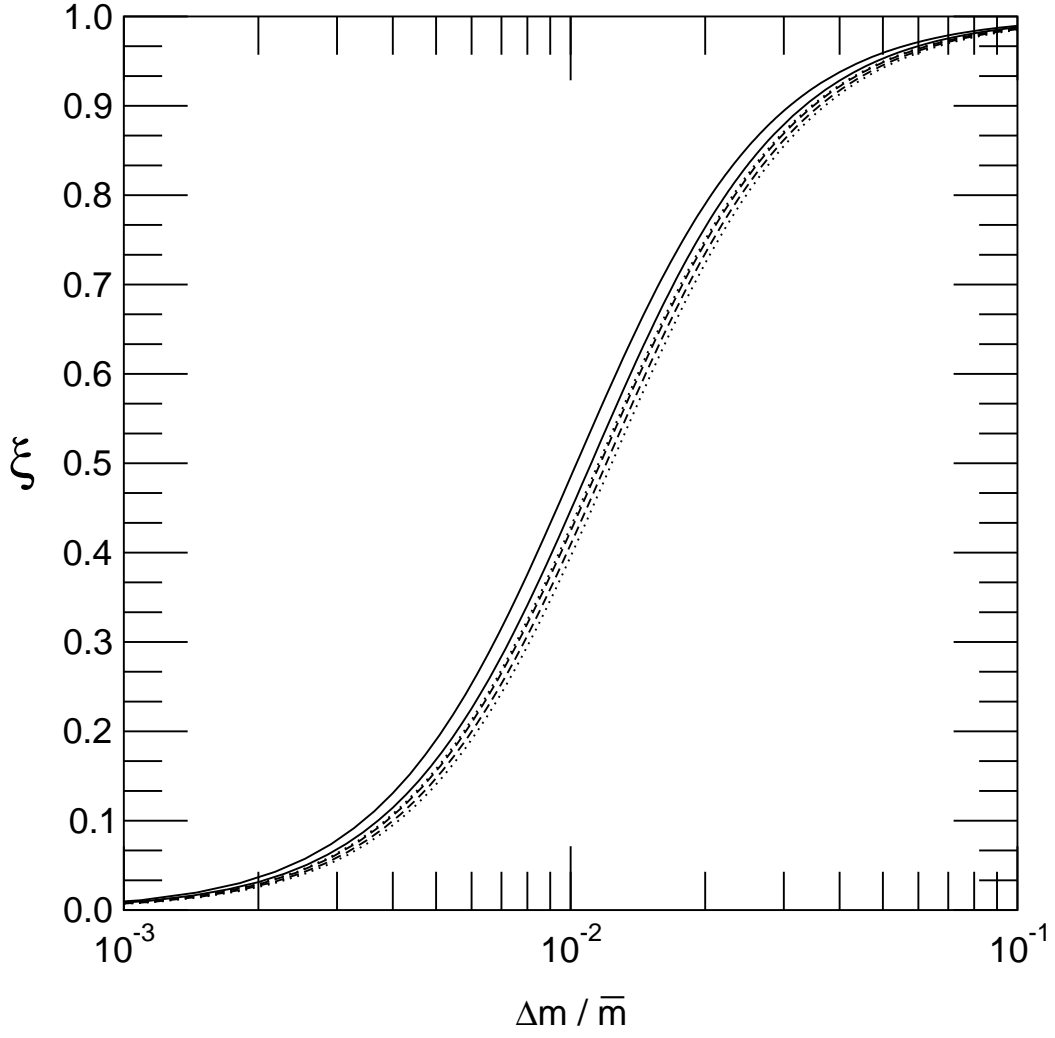


FIG. 4. The L-violating parameter ξ defined in eq. (6) as a function of the dimensionless ratio $\Delta m / \bar{m}$. The various curves refer to the parameters used in Fig. 3 with the same notation.

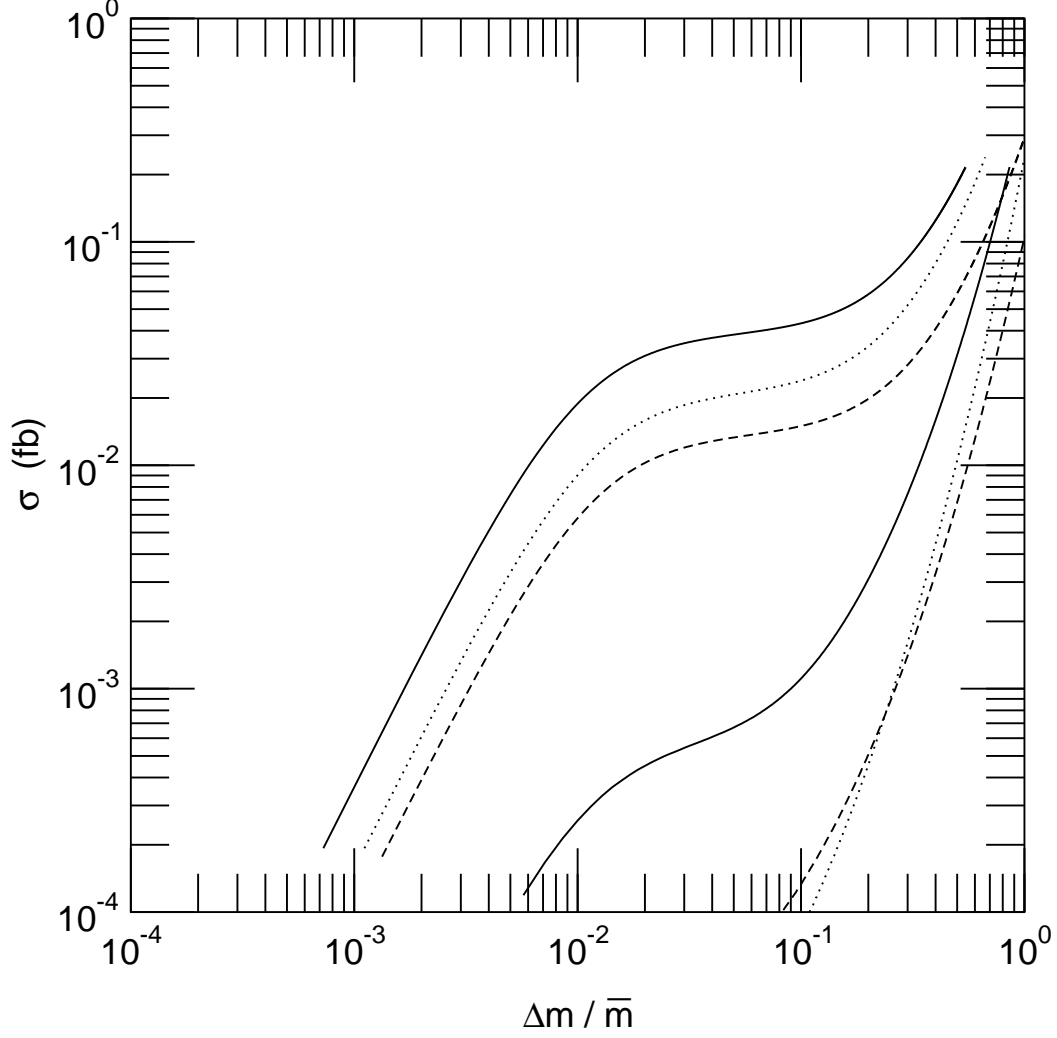


FIG. 5. Cross-section for the wrong sign charged lepton signal stemming from the chargino-associated sneutrino production depicted in Fig. 1-I and 1-II as a function of the ratio $\Delta m / \bar{m}$. The curves correspond to the parameters $\sqrt{s} = 500$ GeV, $\bar{m} = 275$ GeV (parameter set A, upper solid line); $\sqrt{s} = 500$ GeV, $\bar{m} = 350$ GeV (set A, lower solid line); $\sqrt{s} = 800$ GeV, $\bar{m} = 450$ GeV (set A, upper dashed line); $\sqrt{s} = 800$ GeV, $\bar{m} = 600$ GeV (set A, lower dashed line); $\sqrt{s} = 800$ GeV, $\bar{m} = 450$ GeV (set B, upper dotted line); $\sqrt{s} = 800$ GeV, $\bar{m} = 600$ GeV (set B, lower dotted line). The parameter sets A and B have been defined in tab. I.

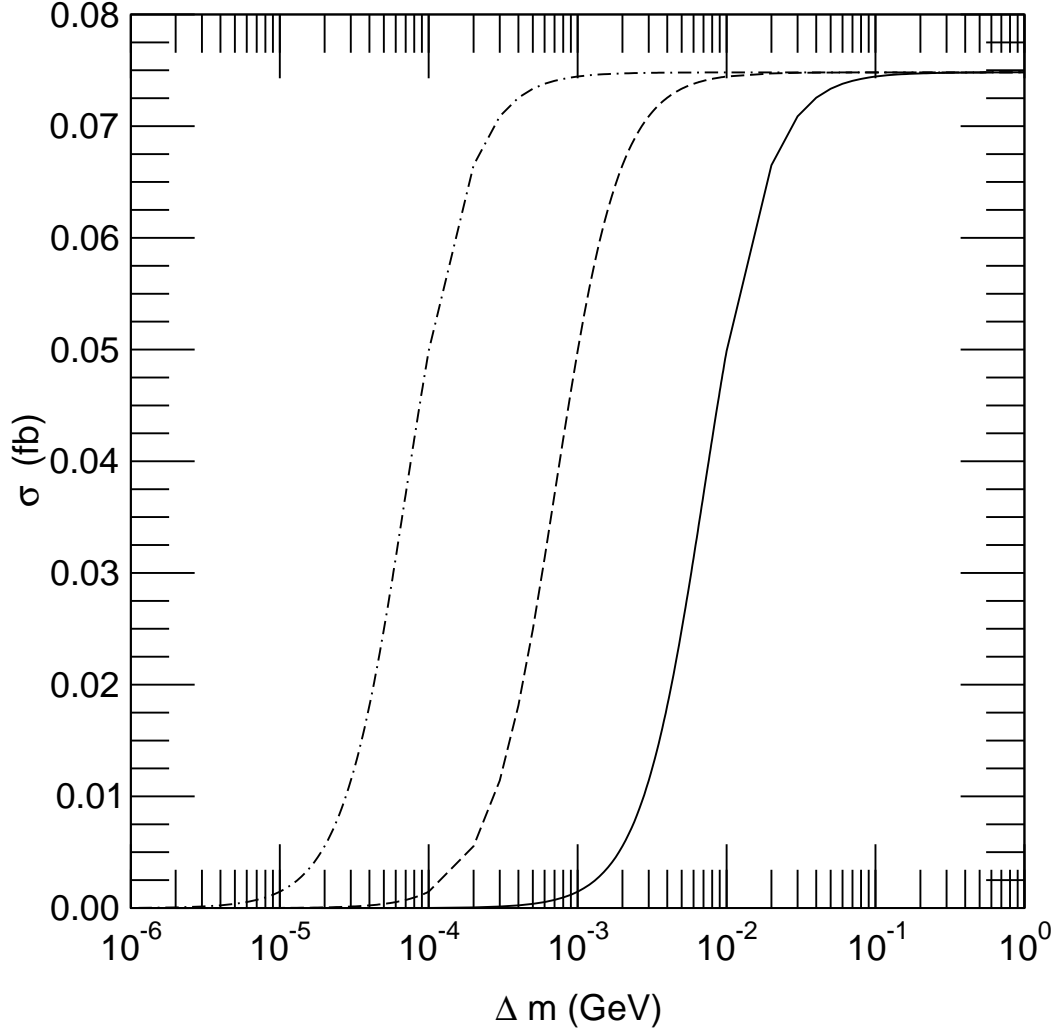


FIG. 6. Cross section of the wrong sign lepton signal for the case of a very small common sneutrino width $\Gamma := \Gamma^{tot}(\tilde{\nu}^1) = \Gamma^{tot}(\tilde{\nu}^2) = \Gamma(\tilde{\nu}^1 \rightarrow \chi^\pm \ell^\mp) = \Gamma(\tilde{\nu}^2 \rightarrow \chi^\pm \ell^\mp)$ and for the parameters (set A; $\sqrt{s}=500$ GeV; $\overline{m}=275$ GeV) in dependence of Δm (in GeV). The solid line corresponds to $\Gamma=10$ MeV, the dashed line corresponds to $\Gamma=1$ MeV and the dot-dashed line to $\Gamma=100$ keV. For a neutrino mass of order $\mathcal{O}(1$ eV) ($\Delta m \approx 200$ keV $= 2 \times 10^{-4}$ GeV, see eq. 8) the L-violating signal is of order $\mathcal{O}(0.01$ fb) (dashed line).

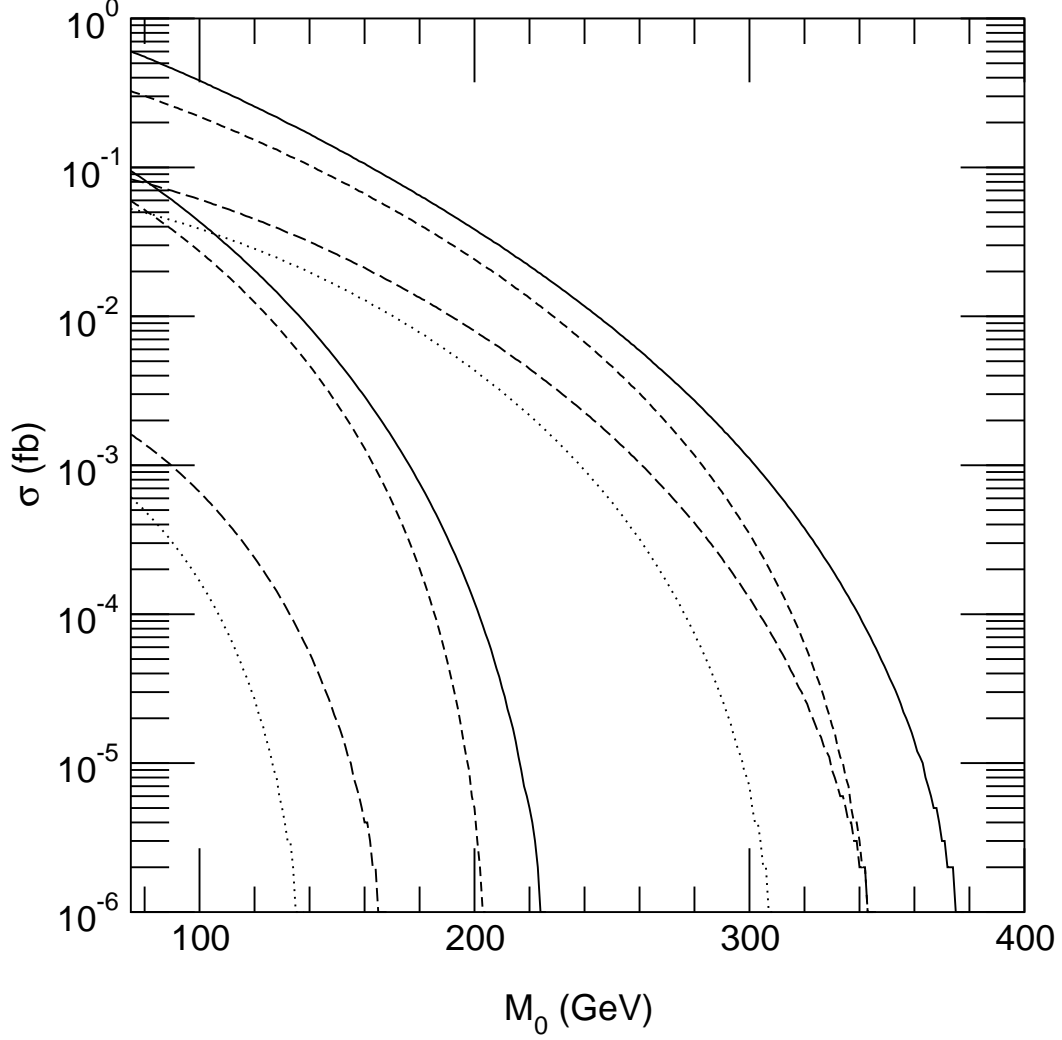


FIG. 7. Cross-section for $e^+\gamma \rightarrow \tilde{\nu}_\ell^N \tilde{\ell}^+ \bar{\nu}_e$ in a mSUGRA scenario as a function of the common scalar mass M_0 , applying the backscattering process (B.S.) eq. (14) and the equivalent photon approximation (E.P.A) eq. (15). The curves correspond to the parameters ($\sqrt{s}=800$ GeV, parameter set A; E.P.S.; upper solid line); ($\sqrt{s}=500$ GeV, set A; E.P.S.; lower solid line); ($\sqrt{s}=800$ GeV, set B; E.P.S.; upper long-dashed line); ($\sqrt{s}=500$ GeV, set B; E.P.S.; lower long-dashed line); ($\sqrt{s}=800$ GeV, set A; B.S.; upper dashed line); ($\sqrt{s}=500$ GeV, set A; B.S.; lower dashed line); ($\sqrt{s}=800$ GeV, set B; B.S.; upper dotted line); ($\sqrt{s}=500$ GeV, set B; B.S.; lower dotted line). The parameter sets A and B have been defined in tab. I (the center of mass energy refers to the electron-positron beam).

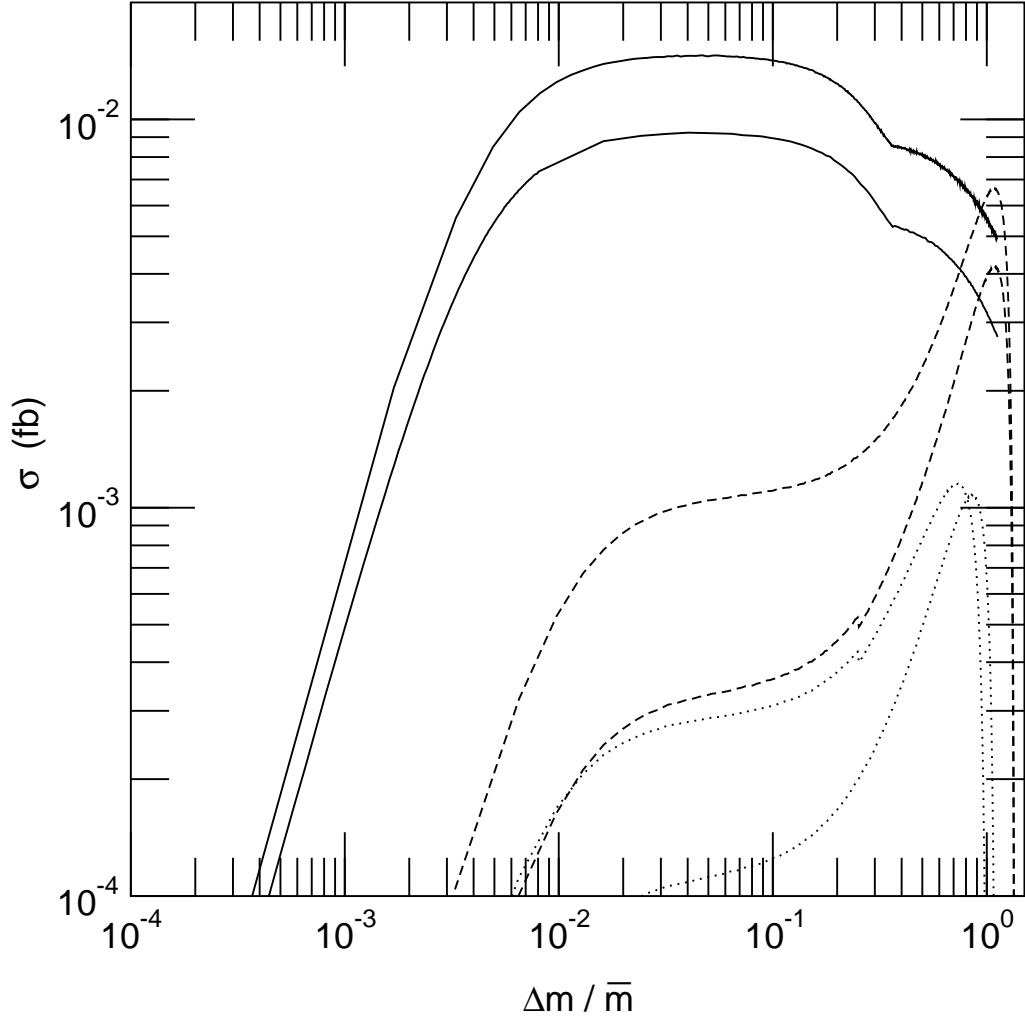


FIG. 8. Cross-section for the wrong sign charged lepton signal stemming from $e^+\gamma \rightarrow \tilde{\nu}_\ell^N \tilde{\ell}^+ \bar{\nu}_e$ (in a mSUGRA scenario) as a function of the ratio $\Delta m/\bar{m}$ applying the backscattering process (B.S.) eq. (14) and the equivalent photon approximation (E.P.A) eq. (15). The curves correspond to ($\sqrt{s}=500$ GeV, $M_0=100$ GeV; parameter set A; E.P.S.; upper solid line); ($\sqrt{s}=500$ GeV, $M_0=100$ GeV; set A; B.S.; lower solid line); ($\sqrt{s}=800$ GeV, $M_0=300$ GeV; set A; E.P.S.; upper dashed line); ($\sqrt{s}=800$ GeV, $M_0=300$ GeV; set A; B.S.; lower dashed line); ($\sqrt{s}=800$ GeV, $M_0=300$ GeV; set B; E.P.S.; upper dotted line); ($\sqrt{s}=800$ GeV, $M_0=300$ GeV; set B; B.S.; lower dotted line). The parameter sets A and B have been defined in tab. I. For $M_0=100$ GeV the data is cut off where the lighter sneutrino becomes lighter than the LSP, the bump corresponds to the value of Δm where the heavier sneutrino is not produced any more.

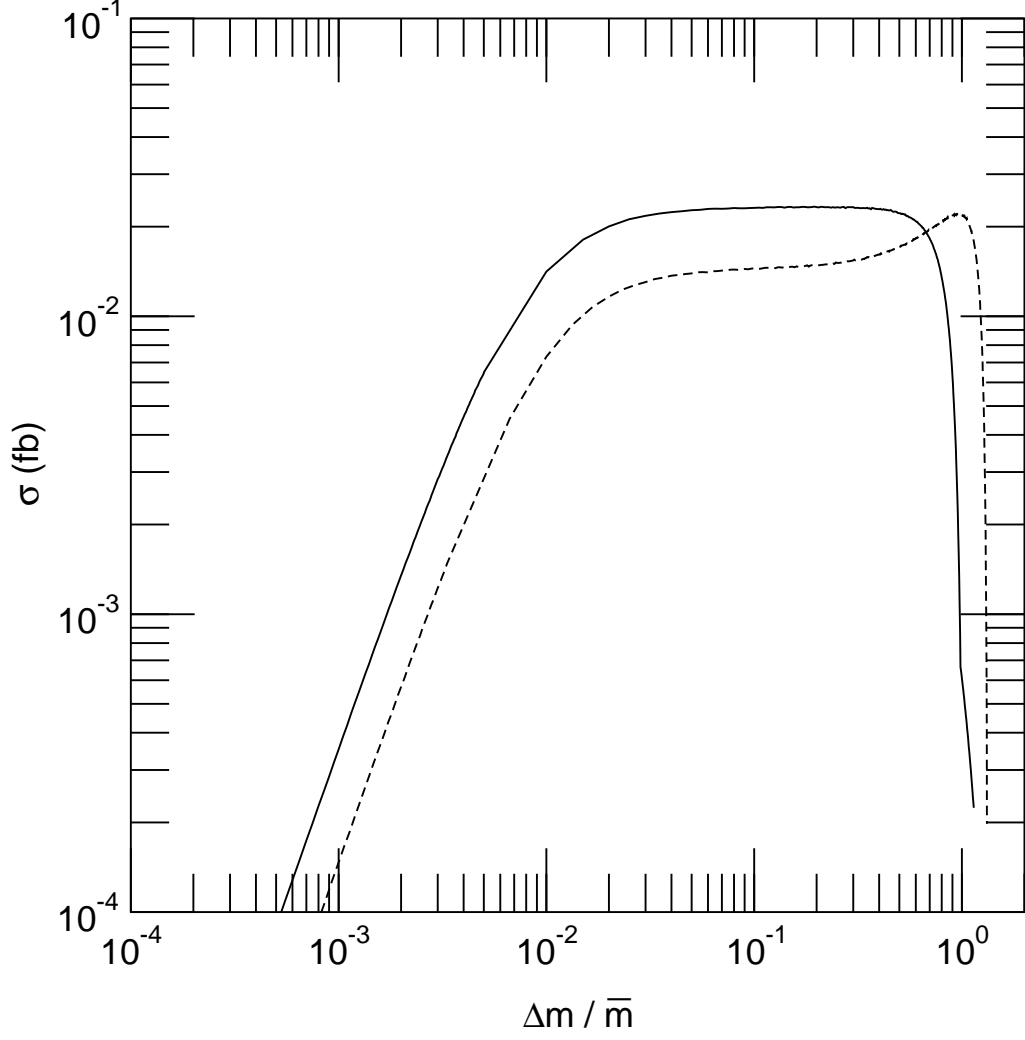


FIG. 9. Cross-section for the wrong sign charged lepton signal stemming from $e^+\gamma \rightarrow \tilde{\nu}_\ell^N \tilde{\ell}^+ \bar{\nu}_e$ as a function of the ratio $\Delta m/\bar{m}$ applying the backscattering process (B.S.) eq. (14). No mSUGRA conditions were assumed. The curves correspond to ($\sqrt{s}=500$ GeV, $\bar{m}=200$ GeV; $m_{\tilde{\ell}}=100$ GeV; parameter set A; B.S.; solid line); ($\sqrt{s}=800$ GeV, $\bar{m}=300$ GeV; $m_{\tilde{\ell}}=200$ GeV; parameter set A; B.S.; dashed line); The parameter set A has been defined in tab. I.